MYU Tokyo

S & M 1727

Room-temperature Hermetic Packaging Using Ultrasonic Cu–Cu Bonding with Compliant Rim

Ryo Takigawa,* Keiichiro Iwanabe, Akihiro Ikeda, Takayuki Takao, and Tanemasa Asano

Graduate School of Information Science and Electrical Engineering, Kyushu University, Nishi-ku Motooka 744, Fukuoka 819-0395, Japan

(Received April 23, 2018; accepted July 4, 2018)

Keywords: hermetic packaging, compliant rim, room-temperature Cu–Cu bonding, ultrasonic bonding, MEMS packaging

In this paper, hermetic packaging using room-temperature (RT) Cu–Cu bonding is demonstrated for microsystem packaging. The bonding of the compliant rim made of Cu to electroplated Cu was performed with ultrasonic assist at RT. Owing to the cone-shaped cross section of the compliant rim, it easily deforms under pressing load with ultrasonic assist and bonds to the counter Cu film at RT. As a result of a simple vacuum test, the air leak rate of the cavity inside the bonded sample was approximately 2×10^{-11} Pa·m^3/s, which may be sufficiently low for applications of vacuum packaging of microdevices.

1. Introduction

Microdevices such as integrated circuits (ICs), micro-electromechanical systems (MEMS), and optical components require hermetic packaging to provide a desired ambient for proper long-term system operation and to protect them from harsh environments.(1–6) In addition, once microdevices are packaged into a single chip or wafer, it is easy to handle them in a subsequent process. In the packaging of microdevices, anodic bonding,(7,8) glass fritting,(9) and solder bonding(10) are the commonly used bonding technologies. However, anodic bonding requires an elevated temperature above 300 °C and a high voltage. Besides, the materials that can be used for anodic bonding are limited to the combination of glass and a conductive material. Glass fritting and solder bonding also require a high-temperature process because of their high melting points. The high-temperature process may degrade the performance of the sealed devices and constrain not only structural design but also the materials involved.

Recently, metal-to-metal bonding has attracted interest in the three-dimensional (3D) microsystem stacking multilayers of active electronic components because of excellent electrical interconnections and enhanced heat dissipation. In particular, copper (Cu) interconnection using Cu–Cu bonding is one of the key elements for future 3D LSIs because of reduced cost, low resistivity, and superior electromigration tolerance.(11–13) Therefore, the development of room-

*Corresponding author: e-mail: takigawa@ed.kyushu-u.ac.jp
https://doi.org/10.18494/SAM.2018.1967

ISSN 0914-4935 © MYU K.K.
https://myukk.org/

temperature (RT) Cu–Cu direct bonding has been of great importance for not only hermetic packaging but also 3D heterogeneous integrations such as LSI and MEMS integrations.

The direct bonding methods of Cu include thermocompression bonding, surface-activated bonding, and ultrasonic bonding. Thermocompression bonding is a well-known bonding method for metals (e.g., Au–Au[14] and Cu–Cu[15–18]). It is usually performed at elevated temperatures of 250–400 °C to obtain sufficient bonding strength. Compared with Au–Au bonding, Cu–Cu bonding in ambient air is difficult since the Cu surface is easily oxidized. A Cu–Cu metallic bond is formed at the bonding interface by atom diffusion across the oxide layer at a high temperature for a long time. In surface-activated bonding, the RT bonding of Cu[19–21] has been demonstrated for microsystem packaging. A large bonding strength can be achieved by the attractive force between atomically cleaned bonding surfaces using a dry etching process such as argon fast atom beam bombardment. In general, Cu–Cu bonding is performed under ultrahigh vacuum to avoid the reoxidation of the activated surface. Although this bonding method is one of the promising candidates, the bonding surface should be strictly planarized[22] and the bonding environment cannot be chosen freely. Recently, low-temperature Cu–Cu bonding has been achieved using a surface activation process based on the reduction effect with formic acid treatment.[23] Ultrasonic bonding is also an effective method because of its advantages of rapid bonding and low-temperature process.[24–26] The low-temperature Cu–Cu bonding of conventional bumps in ambient air has been investigated using ultrasonic assist with surface treatments.[27]

On the other hand, we have developed metallic compliant bumps that are easier to deform than conventional bumps.[28–31] RT bonding in ambient air has been reported using mechanical caulking with Cu compliant bumps.[28] However, the fabrication cost significantly increases because the slit formation in the counter electrode requires additional photolithography. To reduce the fabrication cost, we have proposed the RT bonding of Cu compliant bumps to a Cu planar electrode with ultrasonic assist.[30,31] Recently, RT vacuum packaging has been demonstrated using compliant rims made of Au with ultrasonic assist.[32] A large Au–Au bonding strength could be achieved, and the ability of the compliant rim was experimentally verified. Therefore, we have focused on compliant rims made of Cu.[33]

In this study, we demonstrated RT hermetic packaging using a Cu compliant rim for microsystem packaging. The RT bonding of an electroplated Cu film to the Cu compliant rim was performed in ambient air with ultrasonic assist. The bonding quality and sealing performance were evaluated by the die shear and hermeticity tests.

2. Materials and Methods

Compliant rims made of Cu were fabricated on 4-inch-diameter Si wafers. Figure 1 shows a schematic illustration of the process of fabricating the Cu compliant rim (top size: 2 μm; base size: 10 μm; height: 9–10 μm). First, a TiW film (thickness: 250 nm) and a Au film (thickness: 80 nm) were deposited by sputtering in sequence on a thermally oxidized Si wafer as a seed layer. Next, a photoresist pattern having undercut holes was formed by photolithography.[32] We used a chemically amplified negative-tone photoresist. After that, Cu electroplating was

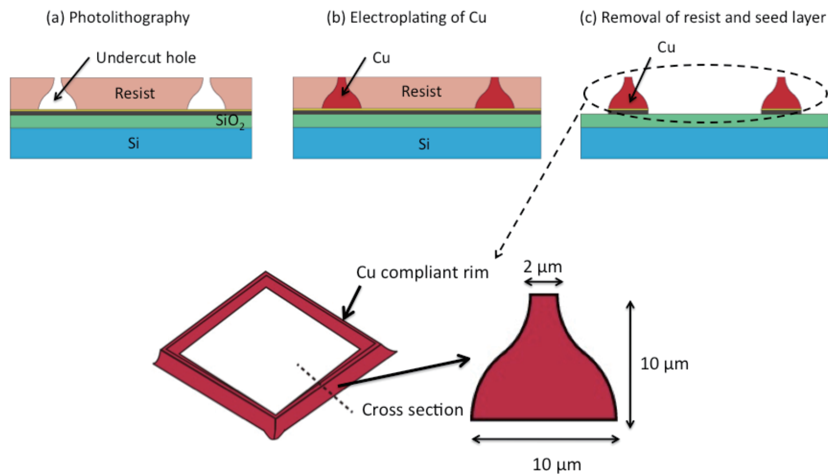

Fig. 1. (Color online) Schematic illustration of fabrication of Cu compliant rim.

applied to fill these undercut holes. The photoresist was removed with acetone. Then, seed layers were removed by ion etching. The Si wafers with Cu compliant rims were cut into 5 × 5 mm^2 chips using a dicing saw. Figures 2(a) and 2(b) show SEM images of the Cu compliant rim on a Si chip. The Cu compliant rim is a square-shaped frame of 500 µm length on one side. On the other hand, Cu sealing frames on glass wafers (width: about 10 µm; height: about 3 µm) were fabricated by standard photolithography and electroplating. The glass wafers were cut into 7 × 7 mm^2 chips using a dicing saw.

Prior to bonding, the chips were chemically cleaned with H_2SO_4, $KHSO_4$, and CH_3COOH to remove contaminants from the Cu surface.[30,31] Subsequently, the RT bonding of glass chips to Si chips was carried out by ultrasonic Cu–Cu bonding in ambient air. Figure 3 shows a schematic illustration of the ultrasonic bonding of Si chips to glass chips. In this experiment, our flip chip bonder equipped with an ultrasonic bonding tool was used.[30–32] The ultrasonic amplitude was 1.5 µm and the ultrasonic frequency was 48.5 KHz. The bonding time was 1.5 s and the pressing load was 40 N/rim.

3. Results and Discussion

Glass chips were successfully bonded on Si chips at RT. A die shear test was performed in order to measure the bonding strength of the bonded samples. The bonding strength was about 3.5 N/rim. Figure 4 shows the bonding strengths obtained from Au–Au and Cu–Cu bondings carried out under the same ultrasonic conditions, namely, an ultrasonic amplitude of 1.5 µm, an ultrasonic frequency of 48.5 KHz, and a bonding time of 1.5 s. In the RT bonding of the electroplated Au film to a Au complaint rim, a large bonding strength was obtained under the pressing load of 10 N. However, for Cu–Cu bonding, a similar bonding strength could not be achieved under the same conditions. When the pressing load was increased to 40 N, a large bonding strength was obtained. Compared with Au–Au bonding, Cu–Cu bonding requires a larger pressing load since Cu is harder than Au. After the bonding with the pressing load of

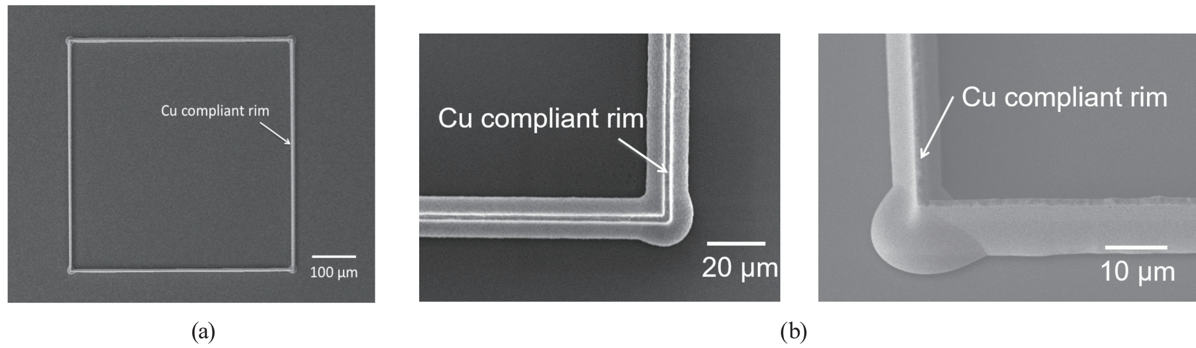

(a) (b)

Fig. 2. (a) SEM image of Cu compliant rim on Si chip and (b) magnified view of (a).

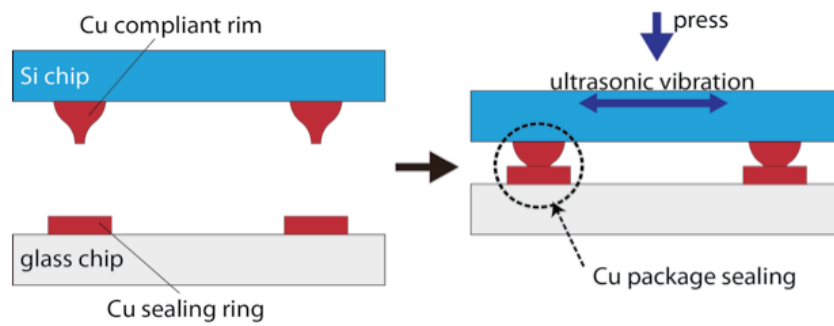

Fig. 3. (Color online) RT Cu–Cu bonding by complaint rim with ultrasonic assist.

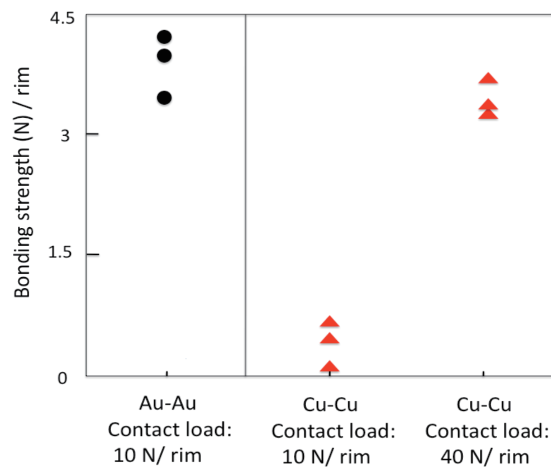

Fig. 4. (Color online) Bonding strengths of Au–Au and Cu–Cu bonds.

40 N, the height of the compliant rim was largely changed from about 9 to about 2 µm. This large deformation may break the oxide and contaminant layers, and bring the two materials into direct contact.

Next, the sealing performance of the bonded samples at room temperature was evaluated. As shown in Fig. 5(a), the water leakage test was performed by immersing the bonded samples

in water. This test is simple and a good indicator of gas leakage.[32] Figure 6(b) shows an optical microscopy image of a sealed area after immersing it in water. The dark and bright areas represent penetrated water and air, respectively. We can clearly see that the water does not penetrate into the sealed Cu package. This result indicates that no leakage can be identified from the sealed Cu package and strong Cu package sealing was achieved.

A simple vacuum test was also performed. A through hole (diameter: 100 μm) inside the sealing frame on a glass chip was formed for the vacuum test. After that, a Si chip was bonded to a glass chip with a through hole. As shown in Fig. 6(a), the cavity inside the package was evacuated using a turbomolecular pump (TMP) through the hole. The pressure in the cavity was approximately 8.7×10^{-6} Pa, which is close to the value obtained from evacuation without the test piece (pressure: 4.6×10^{-6} Pa). After the gate valve was closed, the change in pressure for the cavities was measured using the vacuum gauge. The volume of the vacuum chamber and

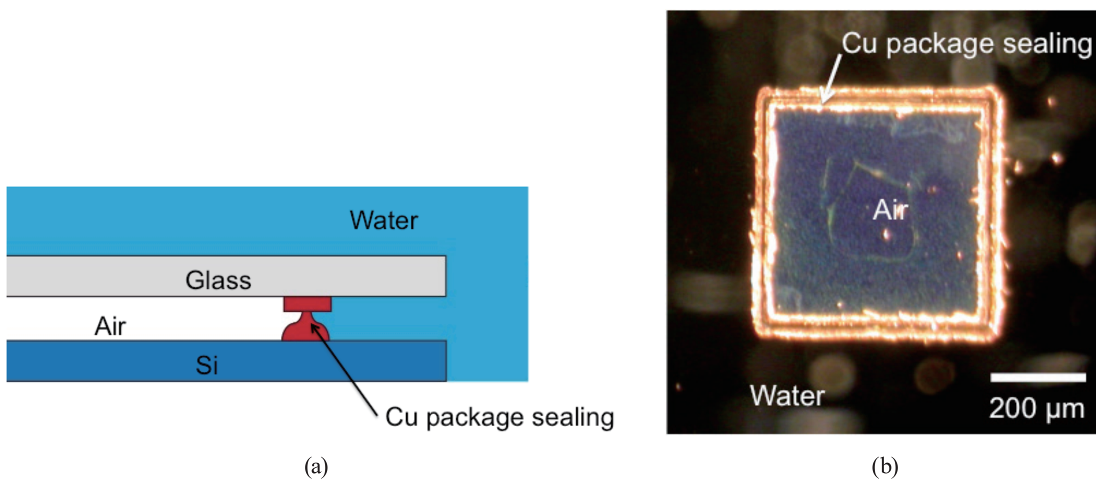

Fig. 5. (Color online) (a) Schematic illustration of water leakage test and (b) optical microscopy image of bonded sample with Cu compliant rim after immersing in water.

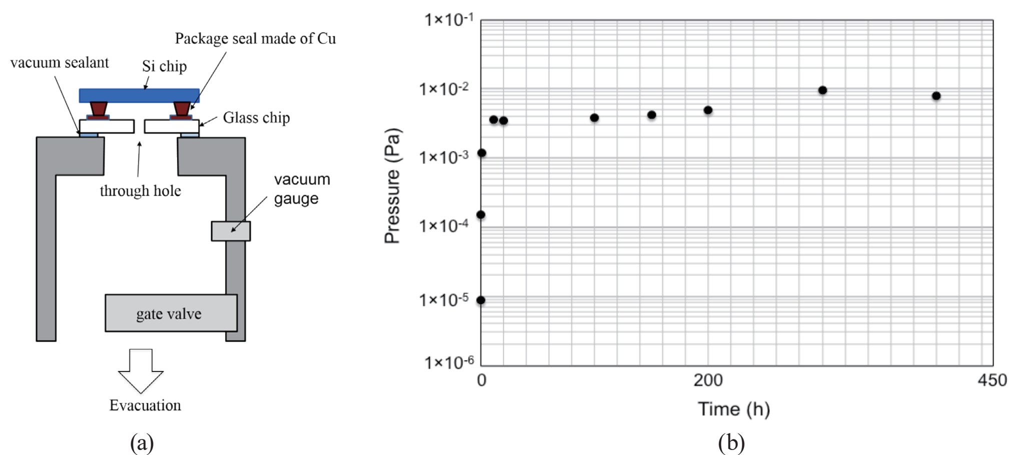

Fig. 6. (Color online) (a) Schematic illustration of vacuum simple test and (b) time dependence of pressure of a vacuum chamber with a test piece.

cavity was approximately 2.5×10^{-3} m^3. Figure 6(b) shows the time dependence of the chamber with the test piece. We can see that the pressure was maintained at less than 1×10^{-2} Pa after 400 h. As calculated from this data, the air leak rate was approximately 2×10^{-11} Pa·m^3/s. This value might be sufficient for the vacuum sealing of microdevices. Our RT Cu–Cu bonding technology indicates the good bonding quality for hermetic packaging.

4. Conclusions

We demonstrate RT hermetic packaging using a Cu compliant rim with ultrasonic assist for microsystem packaging. Strong package sealing was achieved by the Cu–Cu bonding and good sealing performance was confirmed. As a result of the simple vacuum test, the air leak rate is approximately 2×10^{-11} Pa·m^3/s, which may be sufficiently low for use in the vacuum packaging of microdevices. These results show the potentials for 3D heterogeneous integrations such as CMOS and MEMS integrations that require an RT process.

Acknowledgments

This study was supported in part by the A-STEP program (No. AS242Z02927J) of the Japan Science and Technology Agency (JST).

References

1 Y. S. Oh, B. L. Lee, S. S. Baek, H. S. Kim, J. G. Kim, S. J. Kang, and C. M. Song: Sens. Actuators, A **64** (1998) 51.
2 R. Gooch, T. Schimert, W. McCardel, and B. Ritchey: J. Vac. Sci. Technol., A **17** (1999) 2295.
3 B. Lee, S. Seok, and K. Chun: J. Micromech. Microeng. **13** (2003) 663.
4 M. Esashi: J. Micromech. Microeng. **18** (2008) 073001.
5 S. Yamamoto, E. Higurashi, T. Suga, and R. Sawada: J. Micromech. Microeng. **22** (2012) 055026.
6 Y. Kurashima, A. Maeda, R. Takigawa, and H. Takagi: Microelectron. Eng. **112** (2013) 52.
7 Y. S. Lee and K. D. Wise: IEEE Trans. Electron Devices **29** (1982) 42.
8 H. Henmi, S. Shoji, Y. Shoji, K. Yoshimi, and M. Esashi: Sens. Actuators, A **43** (1994) 243.
9 R. Knechtel: Microsyst. Technol. **12** (2005) 63.
10 D. Sparks, G. Queen, R. Weston, G. Woodward, M. Putty, L. Jordan, S. Zarabadi, and K. Jayakar: J. Micromech. Microeng. **11** (2011) 630.
11 M. Koyanagi, H. Kurino, K. W. Lee, K. Sakuma, N. Miyakawa, and H. Itani: IEEE Micro **18** (1998) 17.
12 C. A. Bower, D. Malta, D. Temple, J. E. Robinson, P. R. Coffinan, M. R. Skokan, and T. B. Welch: Proc. Electronic Components and Technology Conf. (2006) 399.
13 M. Motoyoshi and M. Koyanagi: J. Instrum. **4** (2009) P03009.
14 C. H. Tsau, S. M. Spearing, and M.A. Schmidt: IEEE/ASME J. Microelectromech. Syst. **11** (2002) 641.
15 P. Garrou, C. Bower, and P. Ramm: Handbook of 3D Integration: Technology and Application of 3D Integrated Circuits (Wiley-VCH, Weinheim, 2008) p. 475.
16 C. S. Tan, J. Fan, D. F. Lim, G. Y. Chong, and K. H. Li: J. Micromech. Microeng. **21** (2011) 075006.
17 J. Fan, D. F. Lim, L. Peng, K. H. Li, and C. S. Tan: Electron. Solid-State Lett. **14** (2011) H470.
18 L. Peng, L. Zhang, H. Y. Li, and C. S. Tan: IEEE Trans. Electron Devices **21** (2013) 1444.
19 T. H. Kim, M. M. R. Howlader, T. Itoh, and T. Suga: J. Vac. Sci. Technol. **21** (2003) 449.
20 A. Shigetou, T. Itoh, M. Matsuo, N. Hayasaka, K. Okumura, and T. Suga: IEEE Trans. Adv. Packag. **29** (2006) 218.
21 A. Shigetou, T. Itoh, K. Sawada, and T. Suga: IEEE Trans. Adv. Packag. **31** (2008) 473.
22 H. Takagi, R. Maeda, T. R. Chung, and T. Suga: Jpn. J. Appl. Phys. **37** (1998) 4197.

23 W. Yang, M. Akaike, and T. Suga: IEEE Trans. Components Packag. Manuf. Technol. **4** (2014) 951.
24 K. Tanida, M. Umemoto, Y. Tomita, M. Tago, R. Kajiwara, Y. Akiyama, and K. Takahashi: Jpn. J. Appl. Phys. **42** (2003) 2198.
25 T. Zoumpoulidis, J. Van Delft, M. D. Wild, P. E. M Kuijpers, P. D. Graaf, R. Mauczok, K. Bartek, N. Klee, and R. Dekker: 33rd IEEE /CPMT Int. Electronics Manufacturing Technology Symp. (2008) 1.
26 J. Kim, B. Jeong, M. Chiao, and L. Lin: IEEE Trans. Adv. Packag. **15** (2009) 461.
27 J. L. Jo, J. H. Lee, J. G. Lee, S. H. Jeon, J. M. Kim, Y. E. Shin, J. H. Moon, C. D. Yoo, and S. B. Jung: Jpn. J. Appl. Phys. **48** (2009) 07GA07.
28 N. Watanabe, T. Kojima, and T. Asano: IEDM Tech. Dig. (2005) 687.
29 N. Watanabe and T. Asano: Appl. Phys. Express **4** (2011) 016501.
30 L. Qiu, A. Ikeda, K. Noda, S. Nakai, and T. Asano: Jpn. J. Appl. Phys. **52** (2013) 04CB10.
31 L. Qiu, A. Ikeda, and T. Asano: Jpn. J. Appl. Phys. **52** (2013) 068004.
32 R. Takigawa, K. Iwanabe, T. Shuto, T. Takao, and T. Asano: Jpn. J. Appl. Phys. **53** (2014) 06JM05.
33 R. Takigawa, H. Kawano, T. Shuto, A. Ikeda, T. Takao, and T. Asano: 4th IEEE Int. Workshop Low Temperature Bonding 3D Integration (LTB-3D) (2014) 44.